ARTICLES
https://doi.org/10.1038/s41557-020-00558-1
nature chemistry

Catalytic enantiocontrol over a non-classical carbocation

Roberta Properzi[1], Philip S. J. Kaib[1], Markus Leutzsch[1], Gabriele Pupo[1], Raja Mitra[1,3], Chandra Kanta De[1], Lijuan Song[2], Peter R. Schreiner[2] and Benjamin List[1]✉

Carbocations can be categorized into classical carbenium ions and non-classical carbonium ions. These intermediates are ubiquitous in reactions of both fundamental and practical relevance, finding application in the petroleum industry as well as the discovery of new drugs and materials. Conveying stereochemical information to carbocations is therefore of interest to a range of chemical fields. While previous studies targeted systems proceeding through classical ions, enantiocontrol over their non-classical counterparts has remained unprecedented. Here we show that strong and confined chiral acids catalyse enantioselective reactions via the non-classical 2-norbornyl cation. This reactive intermediate is generated from structurally different precursors by leveraging the reactivity of various functional groups to ultimately deliver the same enantioenriched product. Our work demonstrates that tailored catalysts can act as suitable hosts for simple, non-functionalized carbocations via a network of non-covalent interactions. We anticipate that the methods described herein will provide catalytic accessibility to valuable carbocation systems.

The 'non-classical cation controversy'[1] was a prominent chemical dispute of the 20th century and revolved around the structure of the 2-norbornyl cation, a simple bicyclic carbocation made up of seven carbon atoms. The main focus of the debate was defining whether the cation adopted a non-classical, σ-bridged structure (**1**, Fig. 1a) or rather existed as two rapidly equilibrating classical carbocations (**2a**,**b**, Fig. 1a)[1–3]. After decades of research and copious studies on the topic, X-ray crystallography unequivocally confirmed a bridged, non-classical geometry for the controversial ion[4]. Beyond triggering the advancement of contemporary techniques for structural and computational analysis, the long-standing debate played a central role in the realization of carbon–carbon bond σ-donor abilities, outlining the modern bonding theory for carbocations. Namely, classical ions exist as trivalent, planar carbenium ions; whereas non-classical carbonium ions characteristically contain pentacoordinate (or higher) carbon atoms and are adequately described by a three-centre (or multi-centre), two-electron bond (Fig. 1b). Although this dichotomy summarizes the fundamental differences between classical and non-classical ions, a continuum of possibilities lies between these two limiting cases, as a consequence of the varying degrees of charge delocalization that contribute to the stabilization of carbocationic centres through neighbouring group participation[5,6].

Carbocation chemistry has attracted great attention over the past decades and led to fundamental organic transformations and manifold industrial processes[7]. However, achieving stereocontrol in reactions of carbocations is inherently challenging[8,9]. Whereas classical ions have been recently employed in asymmetric catalysis[10–14], stereocontrol over carbonium ions via small-molecule catalysis remains, to the best of our knowledge, unprecedented (Fig. 1b). As for trivalent cations, the major difficulty resides in discriminating between the two faces of their planar structure[8]. Nevertheless, substituents at the carbenium centre can be incorporated to stabilize the vacant *p* orbital and to direct the delivery of a nucleophile. By contrast, we anticipated that controlling the 2-norbornyl cation, a highly reactive, aliphatic carbocation, devoid of ancillary structural elements to serve as discriminating factors, might pose a captivating challenge. Although stereoselective transformations of norbornene[15–19] and enzymatic resolutions of norbornyl derivatives[20] have been established, the formation of a free carbocationic intermediate in these systems has not been invoked. To the best of our knowledge, only a single report describes an antibody-catalysed kinetic resolution of 2-*endo*-norbornyl mesylate to afford the enantioenriched solvolysis product[21]. Hence, we became interested in imparting stereocontrol over the archetypal non-classical ion through asymmetric counteranion-directed catalysis[22]. Indeed, we envisioned that non-covalent interactions, such as ionic interactions, π-effects[23,24] or London dispersion forces[25], would exist in the presence of a large and confined chiral anion and be beneficial for stereoinduction.

Results and discussion

The reverse Winstein experiment. The original experiment by Winstein represented the ideal starting point for our investigations[26]. In his studies, he observed either complete or partial loss of optical activity during the course of acidic solvolysis of 2-*exo*- and 2-*endo*-norbornyl sulfonates to furnish racemic products of the *exo*-configuration (Fig. 1c). In an opposite fashion, we conceived an experiment in which a chiral Brønsted acid enables a diastereo- and enantioselective reaction of racemic starting materials with a suitable nucleophile to furnish the enantiopure product (Fig. 1d). Within this context, we recognized that the nature of the leaving group would be crucial in preventing undesired side or background reactivity; for example, the in situ liberation of an achiral Brønsted acid by-product might enable a competing non-asymmetric reaction. Upon screening a variety of candidates, we identified trichloroacetimidate as an ideal leaving group[27] (Fig. 2a), and subsequently evaluated the catalytic performance of several classes of previously reported chiral Brønsted acids in the presence of ***rac*-4** (Supplementary Section 1.2) and a wide array of nucleophiles. Despite countless combinations being assessed, a general trend

[1]Max-Planck-Institut für Kohlenforschung, Mülheim an der Ruhr, Germany. [2]Institute of Organic Chemistry, Justus Liebig University, Giessen, Germany. [3]Present address: School of Chemical and Biological Sciences, IIT Goa, Ponda, India. ✉e-mail: list@mpi-muelheim.mpg.de

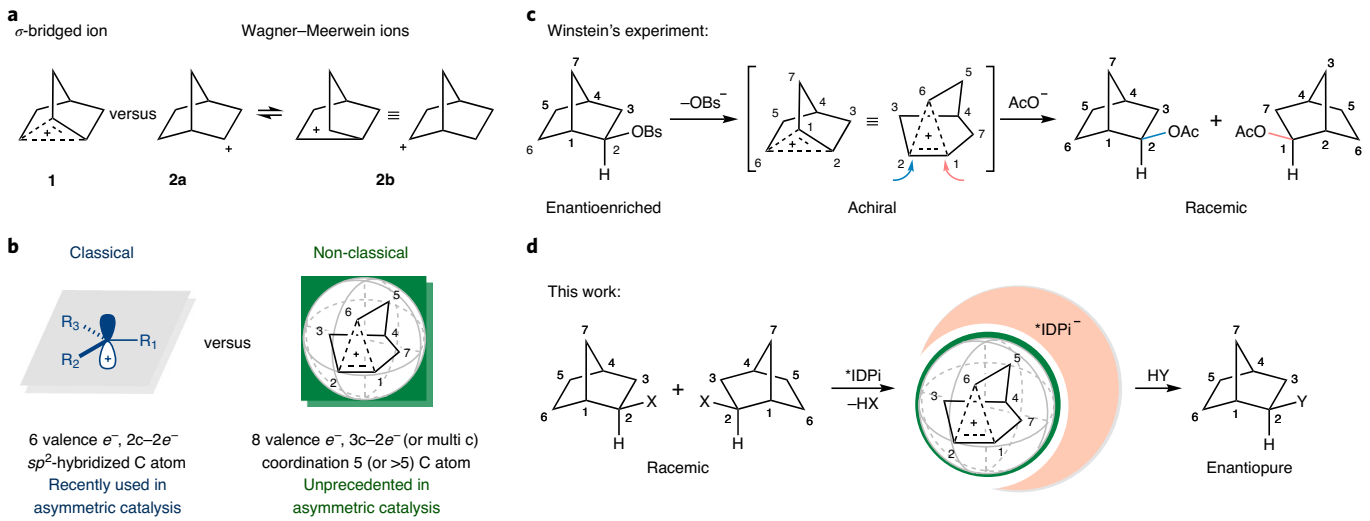

Fig. 1 | The non-classical cation challenge. a, The non-classical cation controversy including the proposal of a bridged, non-classical structure (**1**) and the alternative view of rapidly equilibrating classical cations (**2a,b**). **b**, Electronic and structural features of classical and non-classical cations and their use in asymmetric catalysis. Trivalent classical ions can be described by using two-centre two-electron bonds (2c–2e$^-$), while non-classical ions contain carbon atoms with higher coordination and are electron deficient due to the sharing of two electrons among three centres (3c–2e$^-$) or more. **c**, Winstein's original solvolysis experiment of 2-*exo*-norbornyl sulfonate esters (Bs = $SO_2C_6H_4Br$-*p*); the rate acceleration of ionization compared to the *endo*-isomer and the racemization of products supported the formation of a symmetrical bridged intermediate. **d**, General design of our reverse Winstein experiment; racemic starting materials undergo a diastereo- and enantioselective reaction with a nucleophile of choice to furnish enantiopure products through the association of the 2-norbonyl cation intermediate with a chiral counteranion provided by the catalyst. X and Y represent a generic leaving group and nucleophile, respectively. *IDPi, chiral enantiopure imidodiphosphorimidate catalysts.

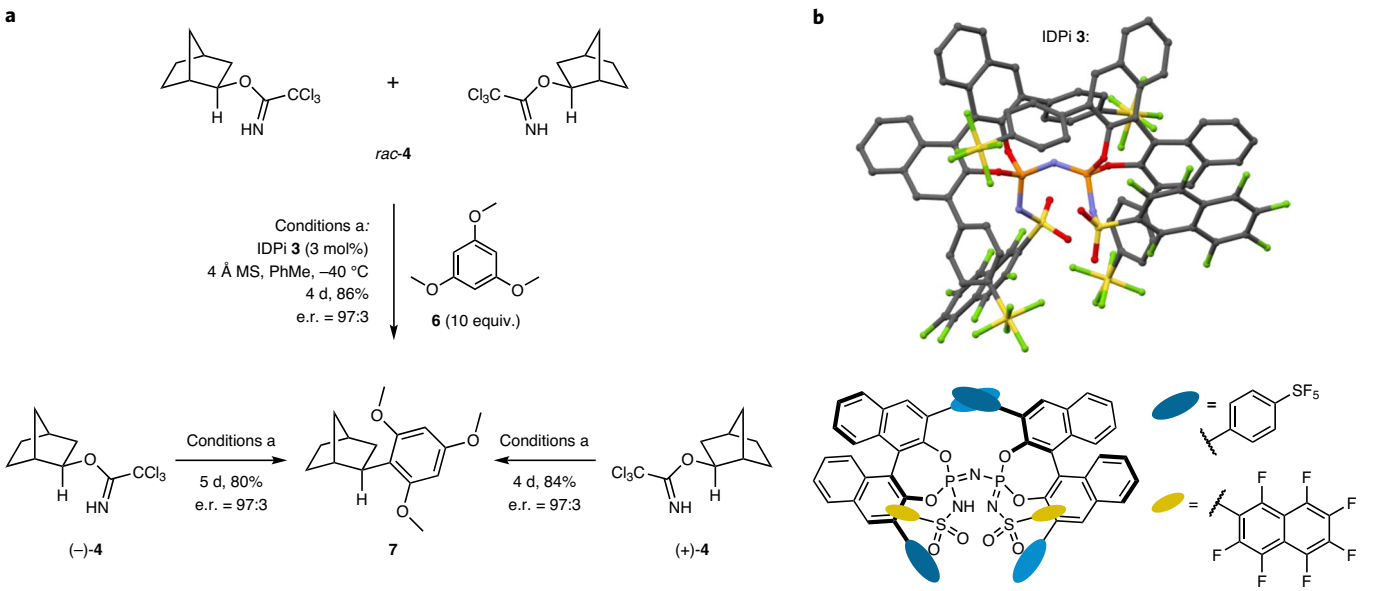

Fig. 2 | IDPi-catalysed enantioconvergent process from *exo*-norbornyl derivatives. a, Product **7** is synthesized from ***rac*-4**, **(–)-4** and **(+)-4** in very good yields and with excellent enantiomeric ratios, regardless of the absolute configuration of the starting material. Identical enantiomeric ratio values of product **7** suggest the participation of a common cationic intermediate. All reactions reached complete conversion of starting material **4** within the depicted reaction times. All yields are those of isolated compounds. Absolute configurations of the single enantiomers of **4** were assigned by optical rotation measurements, on the basis of literature correlations, upon cleavage of the trichloroacetimidate group (Supplementary Section 1.3.4). Enantiomeric ratios were determined by HPLC using a chiral stationary phase. The absolute configuration of **7** was determined by single-crystal X-ray diffraction. Reactions were performed with 0.1–0.2 mmol of **4** in PhMe (0.1 M) at −40 °C. The incorporation of molecular sieves (MS) was only beneficial to the yield, but exerted no effect on the enantioselectivity. **b**, Two-dimensional representation and X-ray structure of IDPi catalyst **3** possessing beneficial substitutions for the achievement of optimal enantioselectivity.

emerged for chiral phosphoric acids[28], chiral disulfonimide (DSI)[29], imidodiphosphate (IDP)[30] and iminoimidodiphosphate (iIDP)[31] catalysts, that is, the tendency of the corresponding conjugate bases to react with the 2-norbornyl cation to irreversibly generate alkylation adducts, thus impeding catalytic turnover[32]. In this regard, a distinct improvement was observed when employing our recently

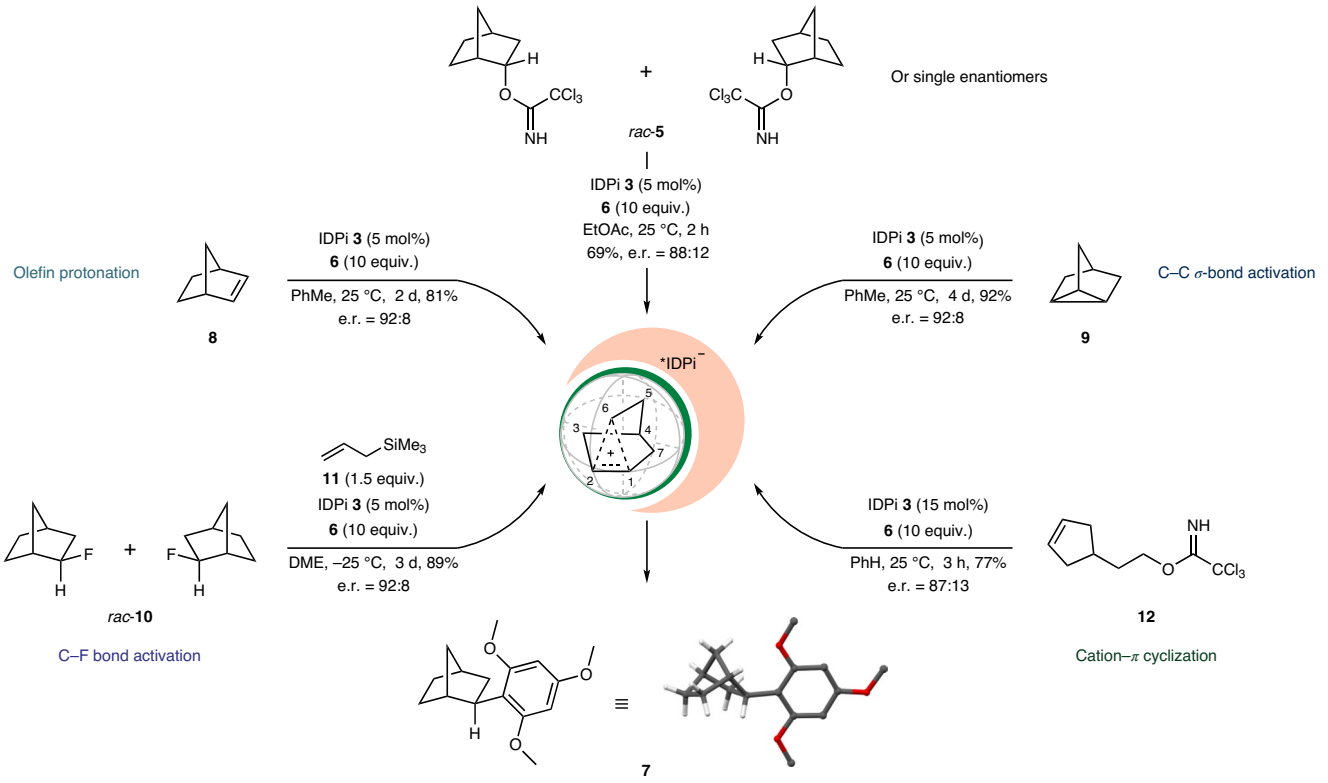

Fig. 3 | IDPi-catalysed synthesis of enantioenriched product from various substrates. Exploration of the active substrate functionalities reveals that various structurally different substrates serve as precursors for the synthesis of enantioenriched product **7**. A reactivity and enantioselectivity comparison with ***rac*-4** suggests the participation of the same 2-norbornyl cation intermediate (Supplementary Section 1.3.5). Reactions were performed on a 0.1–0.15 mmol scale, with concentrations ranging from 0.5 to 0.1 M (Supplementary Section 1.3.5). All reactions reached complete conversion of the starting material in the depicted reaction times. All reported yields are those of isolated compounds. Enantiomeric ratios were determined by HPLC using a chiral stationary phase. DME, 1,2-dimethoxyethane.

developed imidodiphosphorimidate (IDPi) catalysts, which display superior catalytic performance due to the reduced Lewis basicity of the chiral counteranion[33]. Owing to their versatile structural features, which allow for intricate fine tuning of steric and electronic properties, these catalysts demonstrate a marked ability to engage a variety of simple, aliphatic substrates in diverse chemical transformations[34]. We therefore synthesized and evaluated an extensive library of IDPi catalysts in combination with an assortment of nucleophiles. The endpoint of this quest was the identification of two promising motifs capable of delivering product **7** in good yields and enantioselectivities when 1,3,5-trimethoxybenzene (**6**) was employed as nucleophile (Supplementary Table 1). Upon an exhaustive screening of conditions, we selected IDPi **3** (Fig. 2b) to carry out further investigations and found that product **7** can be obtained in very good yield (86%) and excellent enantioselectivity (enantiomeric ratio, e.r. = 97:3) when the reaction between ***rac*-4** and **6** is performed at −40 °C in toluene with a catalyst loading as low as 3 mol% (Fig. 2a, conditions a). Once we ascertained that the racemic *exo*-substrate could successfully engage in an asymmetric carbon–carbon bond-forming reaction, we individually submitted both enantiomers to identical reaction conditions. Congruously, **(−)-4** and **(+)-4** were fully converted to afford the same product in comparable yields and identical enantiomeric ratios (Fig. 2a). We could, however, note a difference in the reaction rates of the two enantiomers, behaviour that was also identified in a more detailed kinetic analysis (Fig. 4b and Supplementary Section 2.1.1). By contrast, the *endo*-norbornyl derivative ***rac*-5** required slightly harsher reaction conditions, only furnishing the product in ethyl acetate at room temperature with a reaction time of two hours. Nevertheless, the product was obtained in good yield and relatively high enantioselectivity (69%, e.r. = 88:12; Fig. 3). Under the same conditions, the *exo*-substrate (***rac*-4**) afforded the product within minutes in similar yield (70%) and an identical enantiomeric ratio of 88:12 (Supplementary Section 1.3.5). These observations correlate well with Winstein's solvolytic studies, in which the *exo*-precursor was found more reactive than the *endo*-isomer by a factor of 350 (refs. [26,35]). The noticeably higher reactivity of the *exo*-norbornyl ester was attributed to the anchimeric assistance offered by the C_1–C_6 bond, which is not correctly aligned in the *endo*-isomer to aid the ionization[36]. Consistent with our approach in the *exo*-case, both *endo*-enantiomers were independently submitted to the reaction conditions to deliver product **7** in 61–69% yield and equivalent enantiomeric ratio (Supplementary Section 1.3.5).

Diversification of the active substrate functionality. Once we demonstrated the feasibility of a diastereo- and enantioconvergent catalytic process from the 2-norbornyl trichloroacetimidate stereoisomers, we were keen to verify if this approach could be extended to other substrates that might lead to the same cationic intermediate. Therefore, we designed diverse routes to enantioenriched product **7**, finding inspiration in the seminal work of Olah et al. (ref. [37]). We first chose to evaluate a direct protonation of norbornene (**8**) by means of our strong chiral Brønsted acid. The asymmetric catalytic Friedel–Crafts alkylation of **6** with norbornene (**8**) smoothly proceeded in toluene at 25 °C to afford **7** in 81% yield and 92:8 enantiomeric ratio (Fig. 3). Encouraged by this reactivity, we attempted to activate hydrocarbon **9** via protonation. Indeed, under the reaction conditions used for the olefinic substrate,

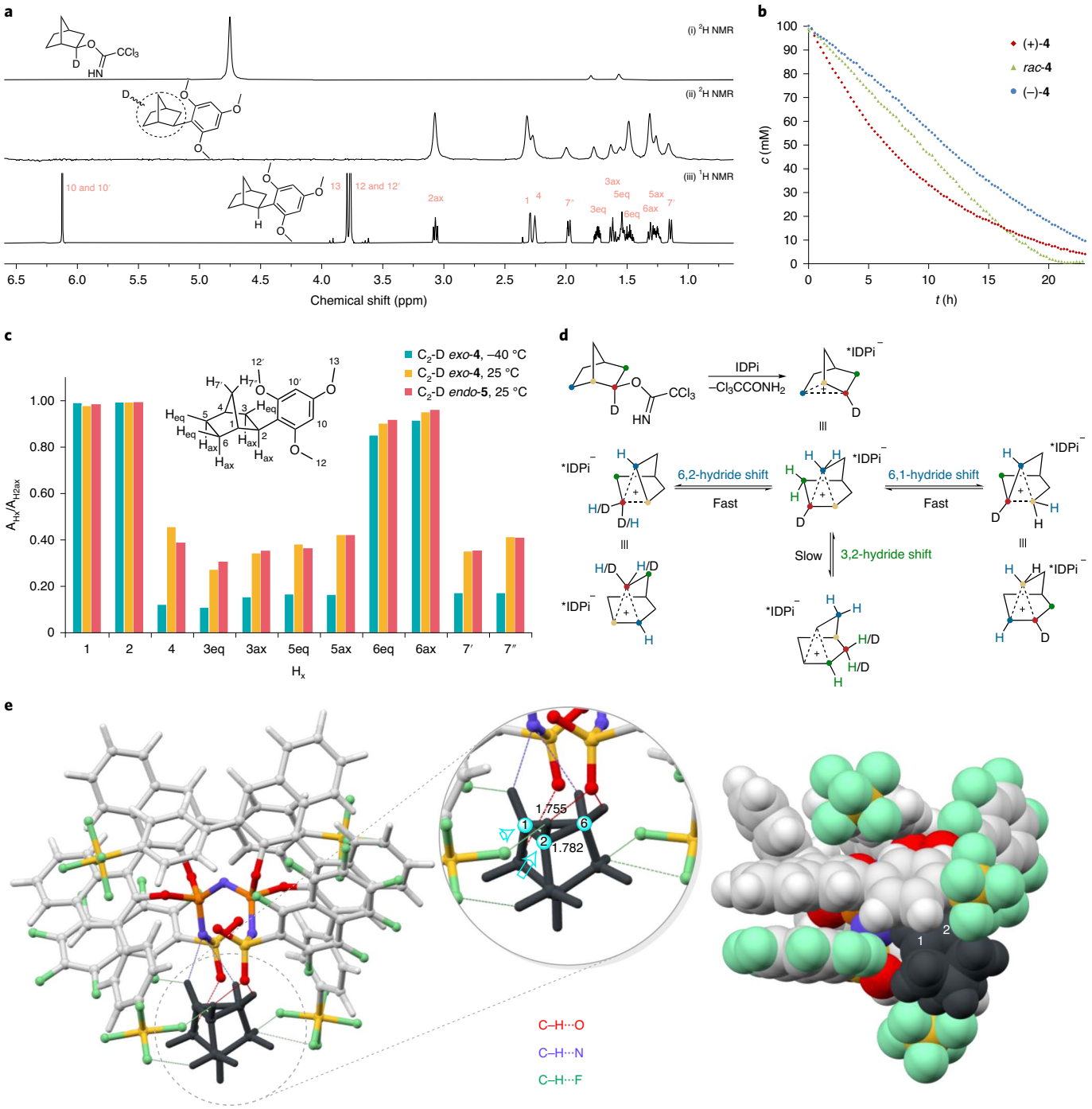

Fig. 4 | Mechanistic investigations. a, Isotope labelling reveals the existence of degenerate hydride shifts responsible for the distribution of the deuterium atom over the norbornyl skeleton. Comparison of NMR spectra qualitatively illustrates the extent of the rearrangements: **(i)** C_2-D-labelled *exo*-norbornyl derivative (C_2-D ***exo*-4**) (^{2}H NMR); **(ii)** deuterated product mixture following the reaction of C_2-D ***exo*-4** in PhMe at 25 °C (^{2}H NMR; Supplementary Section 1.3.6); and **(iii)** product **7** (^{1}H NMR). **b**, Concentration profile of ***rac*-4**, **(–)-4** and **(+)-4** over time shows different reaction rates for the enantiomers of compound **4**; data obtained from ^{1}H NMR for reactions performed with 5 mol% catalyst loading in PhMe at –35 °C (Supplementary Section 2.1.1). **c**, Relative distribution of deuterium in the product for the reactions of C_2-D ***exo*-4** at 25 °C and –40 °C, and from C_2-D ***endo*-5** at 25 °C, reflects the effect of the reaction temperature on fast 6,1,2- and slower 3,2-hydride shifts; comparable distribution profiles for both the *exo*- and the *endo*-isomer indicate the formation of a similar cationic intermediate. Data obtained from ^{2}H NMR line fitting of the individual resonances (Supplementary Section 2.1.3); H_{ax} = pseudo-axial (*endo*) hydrogen atom, H_{eq} = pseudo-equatorial (*exo*) hydrogen atom, H_x = hydrogen atom at position x, A_{Hx} = peak area obtained from ^{2}H NMR line fitting of a given hydrogen atom Hx, AH_{2ax} = peak area obtained from ^{2}H NMR line fitting of the pseudo-axial hydrogen atom in position 2. **d**, Representation of degenerate hydride shifts for the 2-norbornyl cation. Deuteride shifts are not shown; however, they cannot be excluded. **e**, Energetically lowest-lying optimized ball-and-stick model (left, in an orientation comparable to that of **3** in Fig. 2b) and space-filling model (right, in a different orientation) of the non-classical cation complex with the catalyst (level of theory, PBE-D3(BJ)/def2-SVP; for details, see Supplementary Section 2.2).

nortricyclene (**9**) could be converted to product **7** in an excellent 92% yield and equal enantioselectivity of 92:8 (Fig. 3). Notably, under identical reaction conditions, the *exo*-substrate (***rac*-4**) afforded the product in a markedly shorter reaction time in good yields and with the same enantiomeric ratio (e.r. = 92:8). Next, we considered the reaction of 2-*exo*-norbornyl fluoride (***rac*-10**), designing an unprecedented asymmetric transformation in which a chiral silylium-based Lewis acid catalyst is used to cleave the C–F bond, while simultaneously governing the enantioselective addition of the incoming nucleophile to the resulting cationic intermediate[38,39]. As previously demonstrated, IDPi catalysts become highly active and selective 'silylium' Lewis acids upon protodesilylation of a variety of silanes[34], which appoints them as ideal candidates for our experiment. Indeed, under optimized reaction conditions and in the presence of allyltrimethylsilane (**11**), IDPi **3** catalyses the reaction between racemic 2-*exo*-norbornyl fluoride and **6** to furnish product **7** in 89% yield and 92:8 enantiomeric ratio (Fig. 3). Lastly, we chose to challenge our IDPi catalyst in the conversion of substrate **12** to the expected product **7**. This intramolecular cyclization proceeds through the assistance of the π-electrons in the double bond[40], and requires the catalyst to coerce **12** into a bicyclic structure and additionally control the stereochemistry of the nucleophilic addition. Product **7** was successfully obtained in 77% yield and a satisfactory 87:13 enantiomeric ratio when the reaction was carried out in benzene at 25 °C with a moderately increased catalyst loading (Fig. 3).

Mechanistic investigations. The aforementioned transformations were closely investigated by NMR spectroscopy in an attempt to locate and characterize ionic or covalent species, possibly composed of the norbornyl fragment and the IDPi framework. Despite gaining valuable insights into these reactions, in no case could direct evidence for the existence of such intermediates be collected (Supplementary Section 2.1.2). Indeed, these highly reactive, short-lived reaction intermediates are presumably undetectable under the experimental conditions, provided the sensitivity limitations of the spectroscopic method employed. To gather more information, we performed a selective deuterium labelling at C_2 for both ***exo*-4** and ***endo*-5** substrates and submitted these derivatives to the aforementioned reaction conditions. A subsequent analysis of the isotope position in the deuterated analogues of **7** revealed a distribution over all positions of the norbornyl unit when the *exo*-enantiomers were reacted at room temperature (Fig. 4a and Supplementary Section 2.1.3). More specifically, the probability to locate the deuterium isotope was predominant at C_1, C_2 and C_6, while the remaining positions were involved to a minor extent (Fig. 4c, orange). Interestingly, the profile obtained from the reaction of the *endo*-substrate was remarkably similar (Fig. 4c, fuchsia). Lowering the reaction temperature of deuterated ***exo*-4** distinctly hampered the internal rearrangements responsible for locating the isotope over the peripheral positions of the norbornyl fragment, while the incidence at C_1, C_2 and C_6 remained nearly unaffected (Fig. 4c, turquoise). These results point to the existence of a carbocationic intermediate that, in analogy to earlier studies for the non-classical 2-norbornyl cation, undergoes fast 6,1,2- and slower 3,2-hydride shifts (Fig. 4d)[41,42]. Moreover, the consistent isotope distributions and the enantioselective outcomes suggest the participation of a common intermediate in the reaction of all substrates employed.

We also examined the mechanism computationally, using density functional theory (Supplementary Section 2.2), which is rather challenging because of the size of the system, its ion pair nature and the large number of degrees of freedom. Here, we can report on the optimized structure of the energetically lowest-lying ion pair that escaped NMR detection (Fig. 4e). We arrived at this key structure using simulated annealing molecular dynamics simulations in the gas phase to determine the most favourable complex in the optimal conformation. The cation interacts with the catalyst through a variety of rather short C–H···O, C–H···F and C–H···N non-covalent interactions (Fig. 4e, left; dashed lines). Such association with the chiral catalyst counteranion renders positions C_1 and C_2 of the cation diastereotopic, and the respective trajectories of an incoming nucleophile are indicated by arrows (Fig. 4e, left). Additionally, the C_1–C_6 (1.755 Å) and C_2–C_6 (1.782 Å) bond lengths are considerably different, signifying a distorted unsymmetrical geometry of the bridged ion induced by the catalyst. The space-filling model (Fig. 4e, right) emphasizes that the cation is deeply embedded in the catalyst cleft and its surroundings are both sterically confined and highly asymmetric.

Conclusions

In view of these results, we believe we have contributed to the fascinating history of the 2-norbornyl cation, with a modern take on Winstein's original experiment and Olah's pioneering work. Furthermore, IDPi catalysts demonstrated potential for the non-trivial activation of C–C π-bonds and σ-bonds, as well as C–F bonds, while concurrently engaging them in enantioselective transformations. We anticipate that the asymmetric methods described in this paper will find synthetic application in other systems involving cationic intermediates. We also showed that IDPi catalysts are competent Brønsted and Lewis acids in exerting enantiocontrol over simple and highly reactive carbocations, paving the way for the development of transformations that involve non-functionalized carbenium intermediates, as well as carbocation systems structurally prone to non-classical interactions. With the knowledge of recent literature indicating the non-classical character of certain carbocations found in biosynthetic routes[43], we anticipate that our study will provide insights into the desirable understanding of more complex pathways in natural product biosynthesis.

Online content

Any methods, additional references, Nature Research reporting summaries, source data, extended data, supplementary information, acknowledgements, peer review information; details of author contributions and competing interests; and statements of data and code availability are available at https://doi.org/10.1038/s41557-020-00558-1.

Received: 27 December 2019; Accepted: 21 August 2020;
Published online: 28 September 2020

References

1. Weininger, S. J. "What's in a name?" From designation to denunciation—the nonclassical cation controversy. *Bull. Hist. Chem.* **25**, 123–131 (2000).
2. Brown, H. C. *The Nonclassical Ion Problem* 1st edn (Plenum Press, 1977).
3. Schleyer, P. v. R., Mainz, V. V. & Strom, E. T. in *The Foundations of Physical Organic Chemistry: Fifty Years of the James Flack Norris Award* Vol. 1209 ACS Symposium Series Ch. 7, 139–168 (American Chemical Society, 2015).
4. Scholz, F. et al. Crystal structure determination of the nonclassical 2-norbornyl cation. *Science* **341**, 62–64 (2013).
5. Olah, G. A. 100 years of carbocations and their significance in chemistry. *J. Org. Chem.* **66**, 5943–5957 (2001).
6. Olah, G. A. Stable carbocations. CXVIII. General concept and structure of carbocations based on differentiation of trivalent (classical) carbenium ions from three-center bound penta- of tetracoordinated (nonclassical) carbonium ions. Role of carbocations in electrophilic reactions. *J. Am. Chem. Soc.* **94**, 808–820 (1972).
7. Olah, G. A. My search for carbocations and their role in chemistry (Nobel lecture). *Angew. Chem. Int. Ed.* **34**, 1393–1405 (1995).
8. Naredla, R. R. & Klumpp, D. A. Contemporary carbocation chemistry: applications in organic synthesis. *Chem. Rev.* **113**, 6905–6948 (2013).
9. Isomura, M., Petrone, D. A. & Carreira, E. M. Coordination-induced stereocontrol over carbocations: asymmetric reductive deoxygenation of racemic tertiary alcohols. *J. Am. Chem. Soc.* **141**, 4738–4748 (2019).
10. Wendlandt, A. E., Vangal, P. & Jacobsen, E. N. Quaternary stereocentres via an enantioconvergent catalytic S_N1 reaction. *Nature* **556**, 447–451 (2018).

11. Zhao, C., Toste, F. D., Raymond, K. N. & Bergman, R. G. Nucleophilic substitution catalyzed by a supramolecular cavity proceeds with retention of absolute stereochemistry. *J. Am. Chem. Soc.* **136**, 14409–14412 (2014).
12. Braun, M. & Kotter, W. Titanium(IV)-catalyzed dynamic kinetic asymmetric transformation of alcohols, silyl ethers, and acetals under carbon allylation. *Angew. Chem. Int. Ed.* **43**, 514–517 (2004).
13. Brak, K. & Jacobsen, E. N. Asymmetric ion-pairing catalysis. *Angew. Chem. Int. Ed.* **52**, 534–561 (2013).
14. Tsuji, N. et al. Activation of olefins via asymmetric Brønsted acid catalysis. *Science* **359**, 1501–1505 (2018).
15. Brown, H. C., Prasad, J. V. N. V. & Zaidlewicz, M. Hydroboration. 83. Asymmetric hydroboration of representative *cis* disubstituted and heterocyclic olefins with dicaranylboranes of high enantiomeric purity. *J. Org. Chem.* **53**, 2911–2916 (1988).
16. Burgess, K. & Ohlmeyer, M. J. Enantioselective hydroboration mediated by homochiral rhodium catalysts. *J. Org. Chem.* **53**, 5178–5179 (1988).
17. Dorta, R., Egli, P., Zürcher, F. & Togni, A. The [IrCl(diphosphine)]$_2$/fluoride system. Developing catalytic asymmetric olefin hydroamination. *J. Am. Chem. Soc.* **119**, 10857–10858 (1997).
18. Sevov, C. S., Zhou, J. & Hartwig, J. F. Iridium-catalyzed intermolecular hydroamination of unactivated aliphatic alkenes with amides and sulfonamides. *J. Am. Chem. Soc.* **134**, 11960–11963 (2012).
19. Gountchev, T. I. & Tilley, T. D. Hydrosilylation catalysis by C_2-symmetric bis(silylamido) complexes of yttrium. *Organometallics* **18**, 5661–5667 (1999).
20. Eichberger, G., Penn, G., Faber, K. & Griengl, H. Large scale preparation of (+)- and (–)- *endo*-norborneol by enzymatic hydrolysis. *Tetrahedron Lett.* **27**, 2843–2844 (1986).
21. Ma, L., Sweet, E. H. & Schultz, P. G. Selective antibody-catalyzed solvolysis of *endo*-2-norbornyl mesylate. *J. Am. Chem. Soc.* **121**, 10227–10228 (1999).
22. Mahlau, M. & List, B. Asymmetric counteranion-directed catalysis: concept, definition, and applications. *Angew. Chem. Int. Ed.* **52**, 518–533 (2013).
23. Hong, Y. J. & Tantillo, D. J. Perturbing the structure of the 2-norbornyl cation through C–H···N and C–H··· π interactions. *J. Org. Chem.* **72**, 8877–8881 (2007).
24. Hong, Y. J. & Tantillo, D. J. C–H··· π interactions as modulators of carbocation structure—implications for terpene biosynthesis. *Chem. Sci.* **4**, 2512–2518 (2013).
25. Wagner, J. P. & Schreiner, P. R. London dispersion in molecular chemistry—reconsidering steric effects. *Angew. Chem. Int. Ed.* **54**, 12274–12296 (2015).
26. Winstein, S. & Trifan, D. S. The structure of the bicyclo[2,2,1]2-heptyl (norbornyl) carbonium ion. *J. Am. Chem. Soc.* **71**, 2953–2953 (1949).
27. Overman, L. E. Thermal and mercuric ion catalyzed [3,3]-sigmatropic rearrangement of allylic trichloroacetimidates. The 1,3 transposition of alcohol and amine functions. *J. Am. Chem. Soc.* **96**, 597–599 (1974).
28. Akiyama, T. & Mori, K. Stronger Brønsted acids: recent progress. *Chem. Rev.* **115**, 9277–9306 (2015).
29. James, T., van Gemmeren, M. & List, B. Development and applications of disulfonimides in enantioselective organocatalysis. *Chem. Rev.* **115**, 9388–9409 (2015).
30. Čorić, I. & List, B. Asymmetric spiroacetalization catalysed by confined Brønsted acids. *Nature* **483**, 315–319 (2012).
31. Liu, L., Kaib, P. S. J., Tap, A. & List, B. A general catalytic asymmetric Prins cyclization. *J. Am. Chem. Soc.* **138**, 10822–10825 (2016).
32. Fabbri, D., Delogu, G. & de Lucchi, O. Thiophosphonates of 1,1-binaphthol as chiral equivalents of H_2S. Preparation of 2-mercaptonorbornanes and 2-mercaptonorbornenes. *Tetrahedron Asymmetry* **4**, 1591–1596 (1993).
33. Kaib, P. S. J., Schreyer, L., Lee, S., Properzi, R. & List, B. Extremely active organocatalysts enable a highly enantioselective addition of allyltrimethylsilane to aldehydes. *Angew. Chem. Int. Ed.* **55**, 13200–13203 (2016).
34. Schreyer, L., Properzi, R. & List, B. IDPi catalysis. *Angew. Chem. Int. Ed.* **58**, 12761–12777 (2019).
35. Winstein, S. & Trifan, D. Neighboring carbon and hydrogen. XI. Solvolysis of *exo*-norbornyl *p*-bromobenzenesulfonate. *J. Am. Chem. Soc.* **74**, 1154–1160 (1952).
36. Winstein, S. & Trifan, D. Neighboring carbon and hydrogen. X. Solvolysis of *endo*-norbornyl arylsulfonates. *J. Am. Chem. Soc.* **74**, 1147–1154 (1952).
37. Olah, G. A., White, A. M., DeMember, J. R., Commeyras, A. & Lui, C. Y. Stable carbonium ions. C. Structure of the norbornyl cation. *J. Am. Chem. Soc.* **92**, 4627–4640 (1970).
38. Amii, H. & Uneyama, K. C–F bond activation in organic synthesis. *Chem. Rev.* **109**, 2119–2183 (2009).
39. Jaiswal, A. K., Prasad, P. K. & Young, R. D. Nucleophilic substitution of aliphatic fluorides via pseudohalide intermediates. *Chem. Eur. J.* **25**, 6290–6294 (2019).
40. Lawton, R. G. 1,5 participation in the solvolysis of β-(Δ^3-cyclopentenyl)-ethyl *p*-nitrobenzenesulfonate. *J. Am. Chem. Soc.* **83**, 2399–2399 (1961).
41. Saunders, M., Schleyer, P. v. R. & Olah, G. A. Stable carbonium ions. XI. The rate of hydride shifts in the 2-norbornyl cation. *J. Am. Chem. Soc.* **86**, 5680–5681 (1964).
42. Olah, G. A., Prakash, G. K. S. & Saunders, M. Conclusion of the classical-nonclassical ion controversy based on the structural study of the 2-norbornyl cation. *Acc. Chem. Res.* **16**, 440–448 (1983).
43. Tantillo, D. J. The carbocation continuum in terpene biosynthesis—where are the secondary cations? *Chem. Soc. Rev.* **39**, 2847–2854 (2010).

Methods

Product **7** was synthesised from ten different starting materials: ***rac*-4**, **(−)-4** and **(+)-4**, ***rac*-5**, (−)-**5** and (+)-**5**, **8**, **9**, ***rac*-10** and **12**. Enantiomeric ratios and chemical yields for compound **7** vary as a function of the reaction conditions, which were optimized according to the functional group reactivity. It should be noted that under the same reaction conditions, various starting materials deliver product **7** with identical enantiomeric ratios and comparable yield. Herein we report a selected experimental method for the preparation of compound **7** starting from ***rac*-4**. Full experimental details for all methods are provided in the Supplementary Information.

Synthesis of 7 from *rac*-4. In a flame-dried flask under Ar, IDPi **3** (12.7 mg, 6.00 µmol, 0.030 equiv.), 1,3,5-trimethoxybenzene (**6**) (336 mg, 2.00 mmol, 10.0 equiv.) and 4 Å molecular sieves (40.0 mg, 200 mg mmol^{-1}) in PhMe (1.5 ml) were cooled to −40 °C. Then, ***rac*-4** (51.3 mg, 0.200 mmol, 1.00 equiv.) in PhMe (500 µl) was slowly added to the suspension and the mixture stirred at −40 °C for 4 d. Et_3N (27.8 µl, 0.200 mmol, 1.00 equiv.) was added, and the mixture was warmed to room temperature and concentrated under reduced pressure. Purification by column chromatography (silica gel, PhMe/hexanes 10:90 to 30:70) afforded **7** (45.0 mg, 86%, e.r. = 97:3) as a colourless solid.

Data availability

The experimental procedures and analytical data supporting the findings of this study are available within the manuscript and its Supplementary Information file. Raw and unprocessed NMR data are available from the corresponding author upon reasonable request. Crystallographic data for compounds **3** (CCDC 1948386) and **7** (crystal 1, CCDC 2021275; crystal 2, CCDC 1948044; crystal 3, CCDC 1948043; crystal 4, CCDC 2021276) can be downloaded free of charge from the Cambridge Crystallographic Data Centre (www.ccdc.cam.ac.uk).

Acknowledgements

Support from the Max Planck Society, the Deutsche Forschungsgemeinschaft (Leibniz Award to B.L. and Cluster of Excellence Ruhr Explores Solvation (RESOLV, EXC 1069)), the European Research Council (Advanced Grant 'C–H Acids for Organic Synthesis, CHAOS'), the Alexander-von-Humboldt Foundation (fellowship to L.S.), and the Fonds der Chemischen Industrie (fellowship to G.P.) is acknowledged. We thank the technicians of our group and all members of the service departments of the Max-Planck-Institut für Kohlenforschung, with a special mention to R. Goddard, N. Nöthling, A. Deege and H. Hinrichs. We thank J. L. Kennemur and L. Schreyer for discussions during the preparation of the manuscript. We are grateful to B. Mitschke for graphical suggestions and all group members that participated in the crowd reviewing process. We acknowledge A. Blond, D. Petkova and M. R. Monaco for their contributions to initial studies.

Author contributions

B.L. and P.R.S. jointly developed the idea of this project; B.L. conceived, directed and oversaw the project; R.P. designed and conducted the experiments with the help of P.S.J.K.; R.P. and M.L. conducted the mechanistic investigations; M.L. performed the spectroscopic experiments and data analysis; G.P. initiated the experimental work and performed early reactivity studies; R.M. and C.K.D. first synthesized IDPi **3**; L.S. carried out the computations; and R.P. and B.L. wrote the manuscript.

Competing interests

B.L., P.S.J.K. and R.P. are inventors on patent WO2017037141 (A1) filed by the Max-Planck-Institut für Kohlenforschung covering the IDPi catalyst class and its applications in asymmetric synthesis.

Additional information

Supplementary information Supplementary information is available for this paper at https://doi.org/10.1038/s41557-020-00558-1.

Correspondence and requests for materials should be addressed to B.L.

Reprints and permissions information is available at www.nature.com/reprints.